

Journal of Design Against Fatigue
https://minerva-aset.com/JDAF

MINERVA ASET

# Design and finite element analysis of S355J2 wing holders on tank wagons

Adnan Gursoy [a], Abdulkadir Duman [a], Oguzhan Erdogan [a], Cagatay Kaptan [a], Mustafa Yasar [b], Kazem Reza Kashyzadeh [c], Okan Unal [d, e, f, *]

[a] *RC Industry R&D Department, Sakarya, Turkey*

[b] *Department of Metal Education, Karabuk University, Karabuk, Turkey*

[c] *Department of Transport, Academy of Engineering, RUDN University, 6 Miklukho-Maklaya Street, 117198 Moscow, Russia*

[d] *Department of Mechanical Engineering, Karabuk University, Karabuk, Turkey*

[e] *Modern Surface Engineering Laboratory (MSELAB), Karabuk University, Karabuk, Turkey*

[f] *CKN Engineering, Project and Consultancy, Technology Development Zone, Karabuk, Turkey*

*P A P E R  I N F O*

*Paper history:*
Received 15 September 2023
Received in revised form 14 October 2023
Accepted 14 October 2023

*Keywords*:
*Wing holder*
*Thickness reduction*
*Finite element analysis*
*Tank wagon*

*A B S T R A C T*

Wagon component failures that occur during service life can be reduced by applying appropriate geometric changes and using optimization techniques. Therefore, crucial changes are being studied to improve design and performance in structures such as connecting parts, braking systems, suspension, and transmission systems. The wing holders also have a load-bearing feature in connecting the body to the chassis. The strength of the wagon, component stabilization, and weight reduction are of great importance during transportation. In this study, finite element analysis was carried out for the novel type wing holders of the tank wagon system designed via simpler and stepless with various thicknesses. The von Mises stresses and total deformations, as finite element results, for the thicknesses of 10 mm, 12 mm, and 14 mm occurred due to the standard of EN 12663-2:2010 for both longitudinal and vertical loading conditions were extracted from the software. Finally, according to the design improvements, a new wing holder model was developed, which can contribute to the reduction of production and assembly costs.

***doi:***

## 1. INTRODUCTION

In recent years, transportation and economic mobility have increased considerably in line with the economic plan frameworks of the countries [1]. The transfer of airline, road and railway vehicles used in the field of transportation has gained much more interest [2]. Moreover, rail transportation is known to be one of the most reliable transportation methods for raw materials, mines, equipment, vehicles, and passengers. Therefore, the transportation of rail vehicles around the world has been an effective business in recent years [3,4]. It has been shown in the studies that the static and dynamic loads force the railway vehicles extensively and cause various failures [5-9]. During transportation, the load-bearing components of the wagons are typically failed therefore they are periodically subjected to a compulsory maintenance process before use [2]. Also, it has been reported that the failures to which the vehicles are exposed are mostly caused by static and dynamic loads, especially in mountainous and climatic conditions. Due to these conditions, wagons are constantly modified with new design applications, and their components are constantly improved in terms of structural capability [10-15].

Prior to the design, development, analysis, and manufacturing of the railway vehicles, the features of the railway line should be examined, and the design criteria of the vehicles should be determined accordingly [16]. The service life of the railway vehicles-components and the comfort of the passengers are more related to the current state of the railway line than the new vehicle design and manufacture [17]. Early and sudden failures caused by vibration and oscillation on the railway lines lead engineers to design and analyze the current state of the line as well as vehicles [18].

Tank wagons are one of the most reliable vehicles that transfer hazardous goods, particularly oil and its derivatives. The development of current tanks and increasing the capacities by novel design approach are gradually crucial due to the massive need on a world scale [11,19,20]. In addition, it is essential that the reliability, durability, and safety are the critical design

*Corresponding Author Email: ounal@karabuk.edu.tr (Dr. O. Unal)

criteria of the tank wagons. Since cracks occur in the critical zone in tanks that have been operating for many years, and generally reveals fatigue characteristics. Therefore, it is required to perform the design, manufacturing, and analysis in terms of stress, loading, strength, safety, and fatigue performance [20]. Tank wagons and equipment are analyzed by static strength and structural stabilization performance. Yield and tensile strengths are determined, and maximum tensile strengths are tested within this framework [21]. Elastic buckling criteria are also considered, and stiffness measurements are performed accordingly. The vehicle is completely subjected to static and fatigue-based analysis and its life is evaluated at the cumulative damage approach [22].
Numerical simulations, particularly in the last decade, have been used as an industrial application that reduces the cost, which is widely used in design, development, and pre-manufacturing analysis [23,24]. Different designs and models that are studied before construction are analyzed by different approaches such as finite element method to determine whether they are safe or not. Therefore, it offers significant advantages in terms of production time and cost. Positive geometric innovations are incorporated into the new design, but the designs may fail due to weak safety features and thus could be altered during re-modelling [25].
The innovation that distinguishes this study from literature studies is not just a tank wagon analysis, but a detailed study with the design modeling and analysis of an intermediate component wing holder that supports the chassis and the tank, which is among the most critical components of the tank wagon. Although there are studies on tank wagon modeling and analysis in the literature, there are no studies on wing holders design, modelling, and analysis. In this study, the simplified novel design of the wing holders which carry and support the petroleum fuel tank were performed and finite element analysis of the wing holders besides full vehicle were conducted. Due to the geometrically complex structure of the wing holder profiles, the wing holders were optimized according to the thickness under the circumference of design improvement and confirmed by finite element analysis.

## 2. NUMERICAL ANALYSIS via FEM

In this study, a new design was carried out by SolidWorks software, a 3D design program, by simplifying the complex geometrical structures of the full wing holders. The wing holder thicknesses are selected as 10 mm, 12 mm, and 14 mm, respectively, according to EN 12663-2 standard. Structural static analysis [25], was performed by ANSYS software that uses the finite element approach, and the results were compared and finally the wing holders were optimized. The FEM simulation is formed by exposing complex loadings in intrinsic shapes and boundary conditions on the geometric model [12]. An element with a certain volume of V surrounded by a surface S and acted by a traction vector $\bar{t}$ on a part of the surface SF. Total potential energy influences the construction of finite element formulation by using variational principle as follows [12]:

$$\pi = \int_V \sigma^T \varepsilon dV - \int_{S_F} u^T \bar{t} dS = 0 \quad (1)$$

where σ is stress vector, $\varepsilon$ is strain vector, and u is displacement vector. The first order variation of the Equation (1) could be organized as:

$$\delta\pi = \int_V \sigma^T \delta\varepsilon dV - \int_{S_F} \delta u^T \bar{t} dS = 0 \quad (2)$$

Via the constitutive equation σ=Dε and strain displacement equation ε=Bu, Equation (2) is transformed to:

$$\delta u^T = \left[\int_V B^T DB dV\right] u - \delta u^T \int_{S_F} N \bar{t} dS = 0 \quad (3)$$

where N is shape function matrix. Equation (3) is the fundamental expression for the discretization in the finite element method and could be transformed to the algebraic equations as:

$$Ku = f \quad (4)$$

where K is the matrix of element stiffness, and f is the surface load vector. The equation could be solved for displacement vector u by using commercial FEM software. ANSYS utilizes FEM code involving linear and nonlinear elements within a very broad range of materials. To determine stresses, displacements, and temperatures etc. the software utilizes complex approaches [12].

### 2. 1. Geometric Model

The Zaes $62m^3$ wagon is designed to carry a load of approximately 25 tons per axle. This tank wagon was modeled with SolidWorks 2020. Figure 1 shows different wing holder models with identical chassis and tank. Figure 1a shows a bent, and relatively thin sheet metal far from a complex wing shape with a thickness of 10 mm, 12 mm, and 14 mm, respectively. Figure 1b shows a relatively thicker wing holder with different cavity layers. The aim of this study is to use a wing holder mechanism with a simple geometry and a lower thickness instead of a thicker wing holder sheet metal observed in Figure 1b.

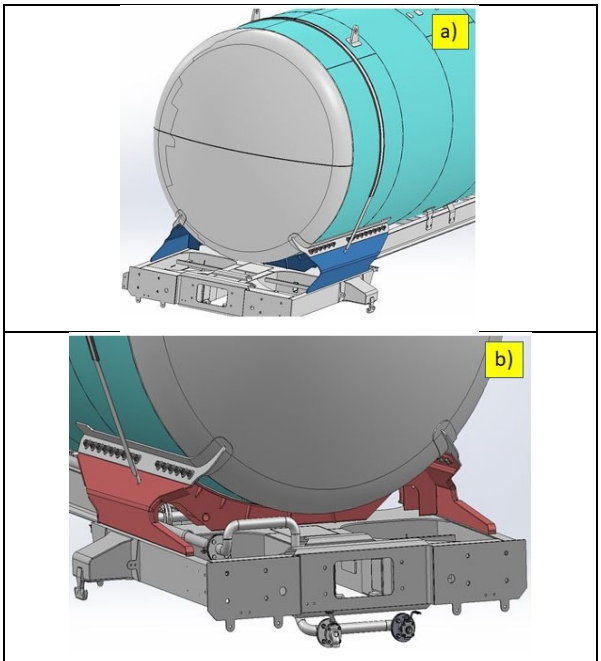



**Figure 1.** Zaes $62m^3$ tank wagon with two different wing holders a) 10-12-14 mm thinner wing holders b) thicker wing holders

### 2. 2. Materials

All platforms of the wagon were made of S355 carbon steel. The chemical composition and mechanical properties were determined by using test specimens obtained from commercially available S355. The chemical composition of S355 is given in Table 1. On the other hand, the mechanical properties of the material are presented in Table 2.

**TABLE 1.** Chemical composition (by wt. %) of S355 carbon steel (Maximum values are reported for all items)

| Element | C | Si | M | P | S | Cu |
|---|---|---|---|---|---|---|
| S355J2 | 0.2 | 0.55 | 1.6 | 0.025 | 0.025 | 0.55 |

**TABLE 2.** Mechanical properties of S355J2 carbon steel

| Property | Magnitude |
|---|---|
| Yield Strength | 355 MPa |
| Ultimate Strength | 630 MPa |
| Modulus of Elasticity | 207 GPa |
| Poisson's Ratio | 0.28 |
| Density | 7850 kg/m$^3$ |

### 2. 3. Meshing Process

In order to perform finite element analysis, shell and solid elements were used depending on the type of component and its application and behavior [26]. The FE model consists of 988,279 elements and the number of 1,262,450 nodes. The tank was designed and modelled via shell elements, while the longitudinal components were solid elements. The Hex Dominant methodology was used to provide more homogenous and well separated mesh type. Figure 2 shows the 3D finite element model of Zaes 62$m^3$ tank wagon.



**Figure 2.** 3D finite element model of Zaes tank wagon

### 2. 4. Mesh Sensitivity Analysis

Mesh sensitivity analysis was conducted to select the optimum mesh size. To this end, the elements were tested according to the maximum von Mises stress. The diagram of stress in terms of element edge size as the results of mesh convergence study is shown in Figure 3. The mesh sensitivity up to 2 mm at regular intervals was investigated by taking the initial element edge length of 20 mm. Deviations up to 12 mm were recorded in the findings. Form Figure 3, the increase in the number of elements after 12 mm did not reveal significant deviations in the stress results. For this reason, the optimum element edge length was determined as 12 mm, considering the analysis time (computational cost). This value also represents the point independent of the element size in the stress analysis.

Figure 4 shows the mesh quality, obtained by the aforementioned analysis, applied to different parts of the wagon. Figure 4a shows the mesh structure in the area where the tank is connected to the chassis, Figure 4b shows the mesh structure applied in the different welded parts of the chassis and profile connections, and Figure 4c shows the mesh structures applied on the wing holders. In finite element analysis, the mesh quality is not deteriorated, even in the complex structures, and generally homogeneity is provided on the wagon cross-sectional zones [27]. The situation contributes the analysis in a way that will not cause large deviations on the results.

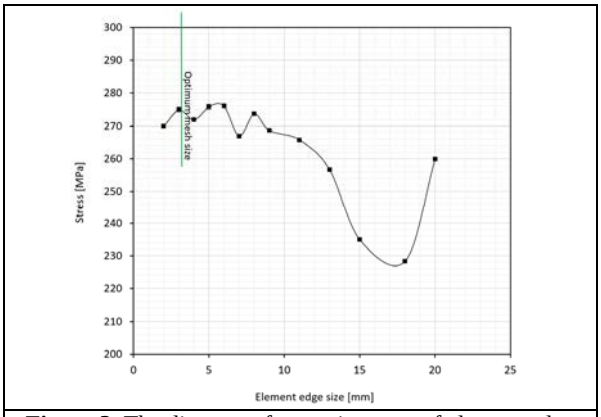



**Figure 3.** The diagram of stress in terms of element edge size as the result of mesh sensitivity analysis

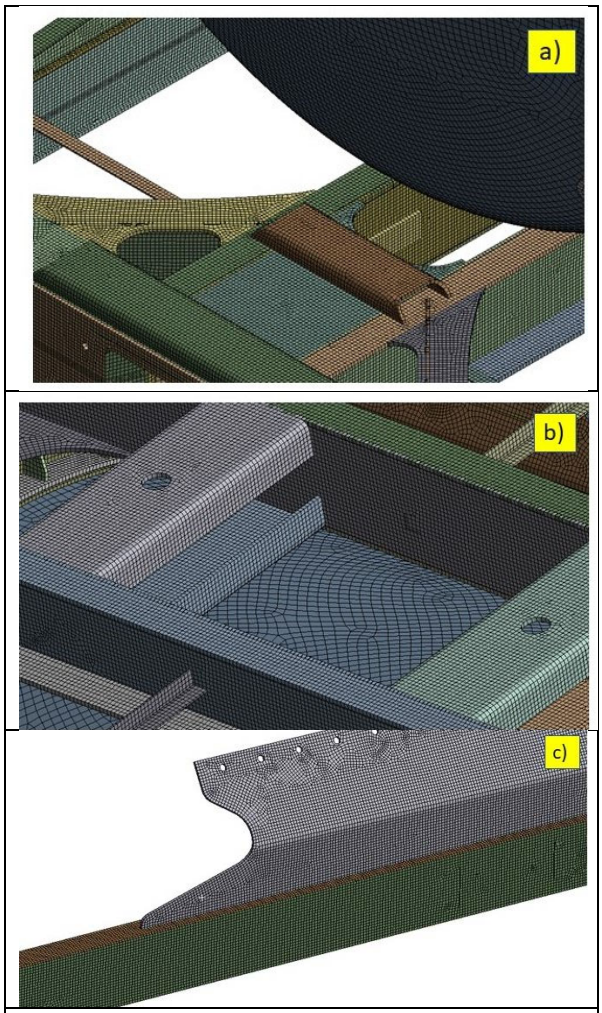



**Figure 4.** Mesh structures of different parts of the wagon a) Tank-chassis connection zone b) Chassis profile connection zone c) Wing holder connection zone

## 2. 5. Loading Case

According to the EN 12663-2 standard [22], static loads should be loaded on the wagon body longitudinally and vertically, respectively [14]. The loading conditions impact were assessed independently on the wagon. Jacking application in lifting and the derailment or its repositioning on the rails of the wagon were examined by the finite element method according to the specified standard. Based on this standard, all tests are analyzed according to the full vehicle condition and are applied as 1200 kN compression, 400 kN diagonal compression, 1500 kN tension, and 900 kN compression (-50 mm) in longitudinal loading conditions. In vertical load cases, vertical loading at 1.3g maximum service condition is analyzed on full vehicle lift and full vehicle lift (+10 mm). The precised results are tried to be revealed by including wagon weights in the analysis. The list of applied load conditions is given in Table 3. In addition, the boundary conditions for each loading are given in Table 4.

**TABLE 3.** Loading conditions of the wagon

| Loading types | Details | Stress Value (MPa) |
|---|---|---|
| **Longitudinal static loads** | | |
| 1200 kN Compression | Compression force was applied to the body | |
| 400 kN Diagonal Compression | Diagonal compression force was applied to the buffers | 118.7 |
| 900 kN Compression (Buffer Level -50 mm) | Compression force was applied at buffers height | |
| 1500 kN tension | Tensile load was applied at the coupler level | 195.9 |
| **Vertical static loads** | | |
| 1.3g Vertical Loading | Maximum operating load conditions | |
| Lifting | Lifting at one end | 312.9 |
| Lifting (+10 mm) | Lifting at all point | 274.7 |

## 2.6. Analysis

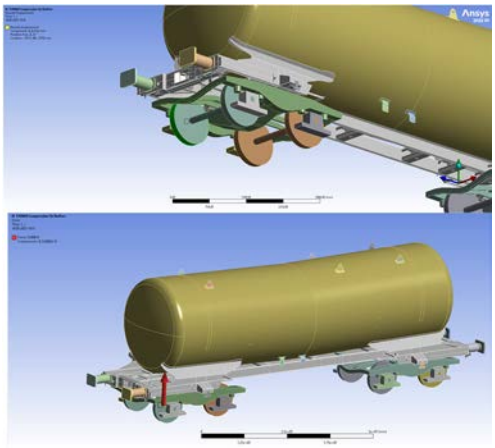
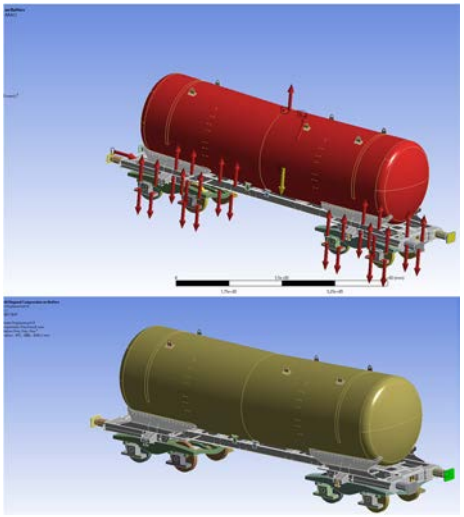
Static structural analysis was performed via Newton-Rapson solver option. The loading conditions were applied as 10% step size. The multilinear materials model was selected for the analysis.

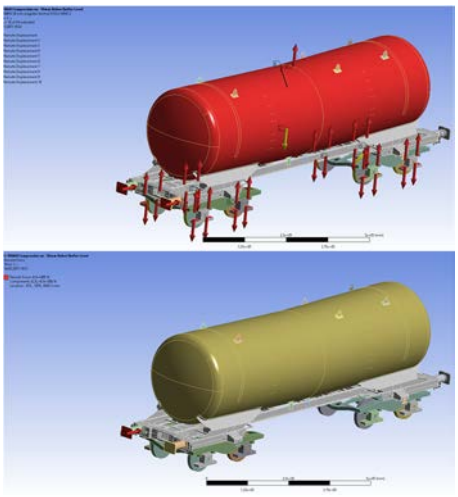
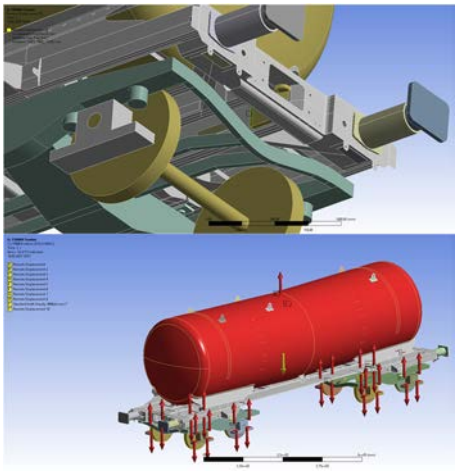
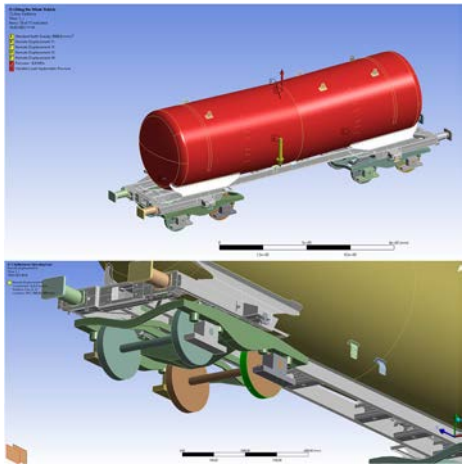
## 3. SIMULATION RESULTS AND ASSESSMENTS

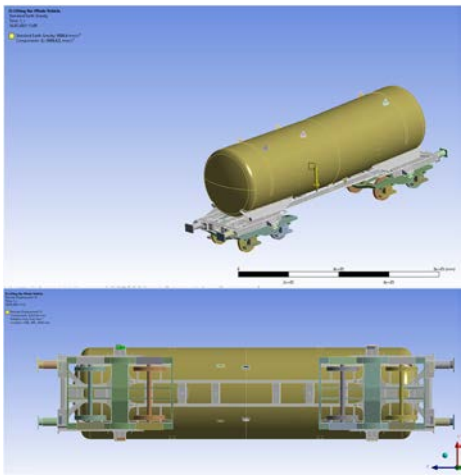
In this study, the approach was carried out to provide weight reduction, reduction of production costs, and fast assembly due to the reduction of the thickness of the wing holders, which provide the side connections of the wagon between the tank and the chassis. The whole system has been reanalyzed and examined in different wing holder thicknesses while the thickness reduction is being performed. Investigations were performed on the whole tank and chassis, but the presented analysis only focuses on reduction the thickness of the wing holder. Eventually, remarkable results were reported in terms of wing holder thickness reduction for the tank, chassis, and entire wagon. The total deformation contour was extracted for whole wagon under different conditions, including compression force of 1200 kN, diagonal compression of 400 kN, and tensile load of 1500 kN, as shown in Figure 5. For the whole wing holder thickness and longitudinal loading conditions, the most critical zones were typically considered to be the wing holder connection and tank cap zones. The safest zone was assessed as the bogie assembly and the upper-middle of the tank was subjected to relatively less load. The most critical deformation occurred at 1200 kN compression,

and a total deformation of 8.73 mm, 8.39 mm, and 8.15 mm was observed for 10 mm, 12 mm, and 14 mm wing holder thicknesses, respectively. Most of the deformations were observed in the bottom of the tank and in the other connection apparatus, especially in the wing holders. Total deformations for all thicknesses of the wing holder are within the range stated in the EN 12663 standard [22].

**TABLE 4.** The boundary conditions for each loading and the loading zones

| Loading types | Boundary Conditions | Loading Zones |
|---|---|---|
| **Longitudinal static loads** | | |
| 1200 kN Compression | Remote Displacements<br>(Rail wheels)<br>Translational movement-x,y,z (0, 0, free)<br>Rotational movement-x,y,z (free, 0, 0)<br>Remote Force 1200 kN<br>(0, 0, -1200 kN)<br>Standard Earth Gravity 9806,6 mm/$s^2$ (0, -9806,6, 0) |  |
| 400 kN Diagonal Compression | Pressure (-0.4 MPa)<br>Remote Displacements<br>(Rail wheels)<br>Translational movement-x,y,z (0, 0, free)<br>Rotational movement-x,y,z (free, 0, 0)<br>Remote Force 400 kN<br>(0, 0, -400 kN)<br>Standard Earth Gravity 9806,6 mm/$s^2$ (0, -9806,6, 0) |  |

| | | |
|---|---|---|
| 900 kN Compression (Buffer Level -50 mm) | Pressure (-0.4 MPa)<br>Remote Displacements (Chassis support)<br>Components (free, free, 0)<br>Rotational movement-x,y,z (free, free, free)<br>Remote Force 900 kN (0, 0, -900 kN)<br>Standard Earth Gravity 9806,6 mm/$s^2$ (0, -9806,6, 0) |  |
| 1500 kN Tension | Pressure (-0.4 MPa)<br>Remote Displacements (Chassis support)<br>Components (free, free, 0)<br>Rotational movement-x,y,z (free, free, free)<br>Remote Force 1500 kN (0, 0, 1500 kN) |  |
| **Vertical static loads** | | |
| 1.3g Vertical Loading | Pressure (-0.4 MPa)<br>Variable Load: Hydrostatic Pressure<br>Remote Displacements (Rail wheels)<br>Translational movement-x,y,z (0, 0, free)<br>Rotational movement-x,y,z (free, 0, 0)<br>Remote Force 2x67600 N (0, 0, 67600 N)<br>Acceleration 12749 mm/$s^2$ |  |

| | | |
|---|---|---|
| Lifting/Lifting (+10 mm) | Remote Displacements<br>(Chassis support)<br>Components (0, 0, 0)<br>Rotational movement-x,y,z (free, free, free)<br>Standard Earth Gravity 9806,6 mm/$s^2$ (0, -9806,6, 0)<br>Pressure (-0.4 MPa)<br>Variable load: Hydrostatic Pressure |  |

Next, the wing holder profile with a thickness of 10 mm was exposed to longitudinal analysis under 1200 kN compression, 400 kN diagonal compression, and 1500 kN tensile load, as well as with 1,3g vertical load. The FE results of this analysis are illustrated in Figure 6. Equivalent stresses occurring on the chassis were determined by FE analysis. In general, maximum equivalent stresses were observed in the components of the chassis connected to the tank zone (in the front and rear parts of the chassis) which were connected by profiles and where the gaps were dense. Regardless of the loading type, stress intensity was noticed in these zones. Maximum equivalent stresses of 389.67 MPa, 381.42 MPa, 436.25 MPa, and 374.73 MPa were obtained for 10 mm wing holder thickness at 1200 kN compression, 400 kN diagonal compression, 1500 kN tensile, and 1.3 g vertical loading conditions, respectively. According to the values, the most critical loading type is 1500 kN longitudinal tensile loading for the chassis, and the most critical location is observed as the wing holder corner turns where the tank was placed. Since the values obtained for the critical points were below the tensile strength according to the EN 12663 standard [22], the outputs were evaluated within the limits of the safe zone.

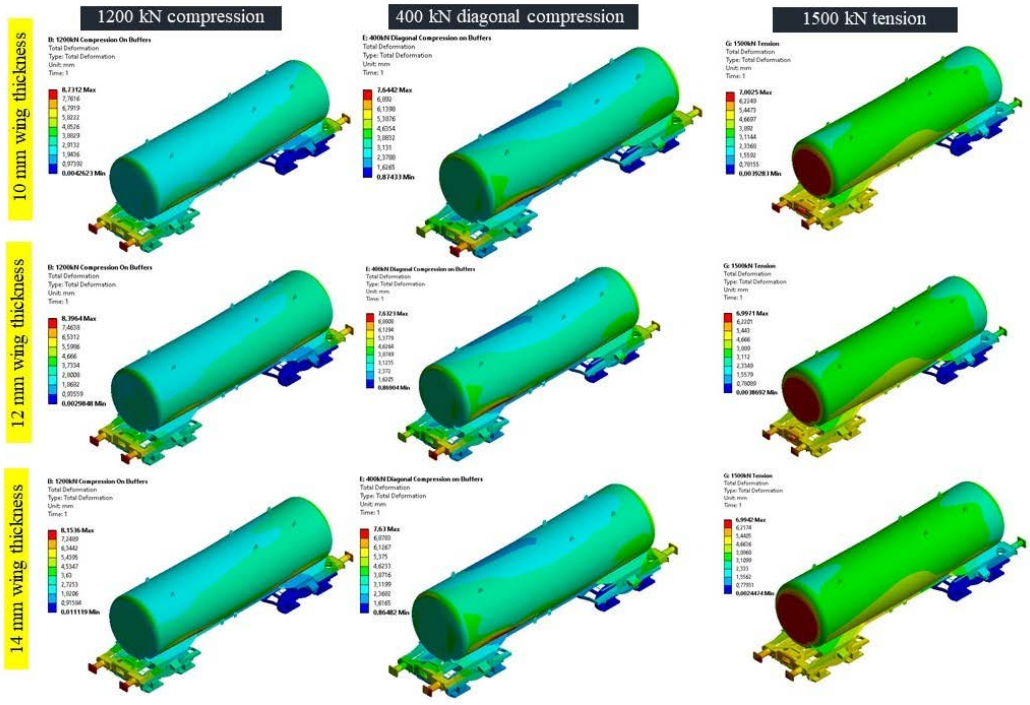



**Figure 5.** The contours of total deformation of the whole wagon related to different wing holder thicknesses after longitudinal loading conditions

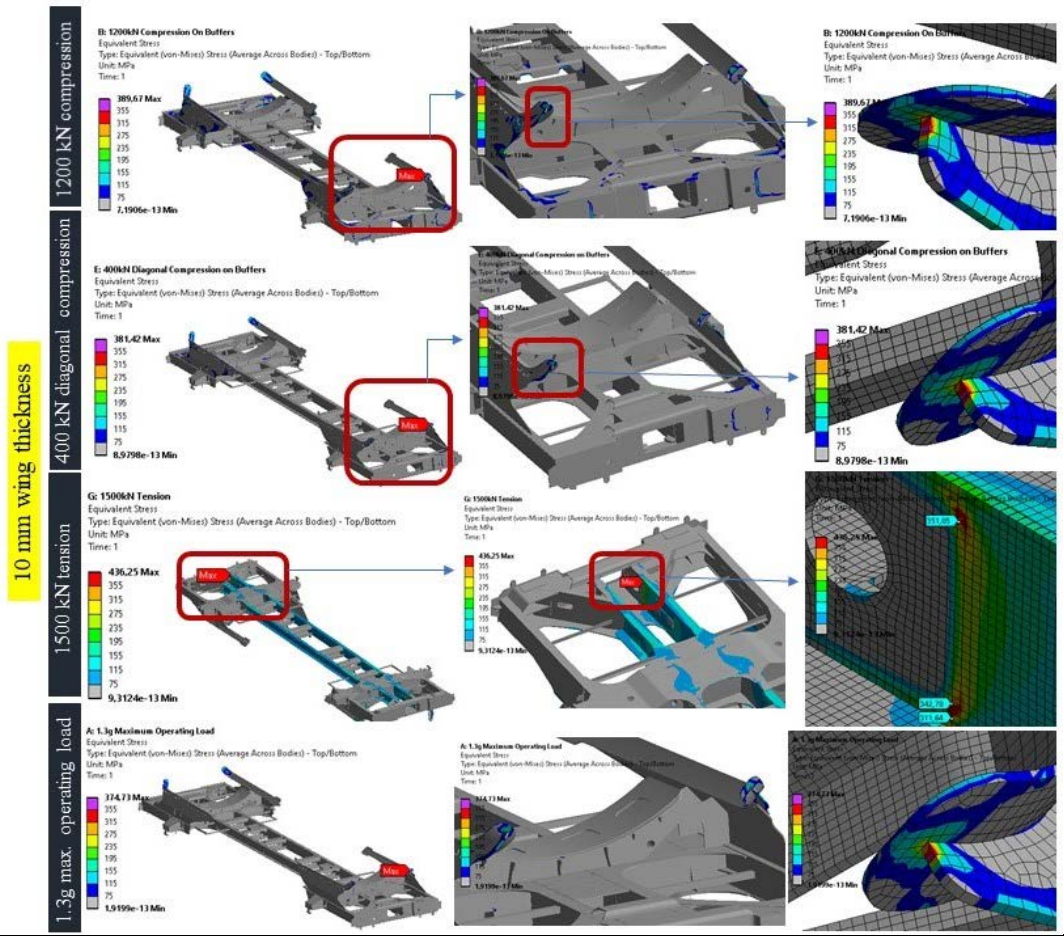



**Figure 6.** Equivalent stress distribution of the chassis under different loadings based on the FE analysis

Figure 7 shows the equivalent stresses in the wagon wing holders after longitudinal load conditions. In longitudinal conditions, 1200 kN compression, 400 kN diagonal compression, 900 kN compression (-50 mm), and 1500 kN tensile loads were applied. For the purpose of wing holder thickness reduction, loads were applied to the wagon platform in each condition of holder thicknesses. The stress concentrations increased in the bolt-nut connection zones, wing bend and corner zones of the wing holders. The most critical regions were similar regions in all wing holder thicknesses. As the thickness decreases, the total surface area ratio of the stress concentration regions increases significantly. Particularly, a proportional increase in stress concentration was observed in the wing holder analysis related to the thickness of 10 mm. The maximum equivalent stress achieved in the wing holder structure was 276.26 MPa, 220.25 MPa, 276.19 MPa, and 194.85 MPa for 1200 kN compression, 400 kN diagonal compression, 900 kN compression (-50 mm), and 1500 kN tensile loading conditions, respectively. According to the results, the maximum equivalent stresses obtained were below the safety coefficient values according to the damage analysis of the materials, and 900 kN compression (-50 mm) was evaluated as the most critical loading condition.

Figure 8 presents the results of stress analysis as a result of vertical loading for the wing holder structure in the entire wagon system by finite element method. According to the results, critical regions appeared likely in longitudinal loading. However, due to vertical loading, the most critical locations have shifted from bolt-rivet connection holes to sheet bending and corner zone. The shift was considered as probable due to the nature of vertical loading condition. Maximum equivalent stresses were reported as 202.58 MPa, 196.61MPa, and 277.42 MPa for a 10 mm thick wing holder at 1.3g maximum service loading, all vehicles lift, and all vehicle lift (+10 mm location) conditions, respectively. According to the results, the most critical condition in vertical loading was observed in the whole vehicle lift (+10 mm location). The evaluated stresses were reasonable since they were lower than the limit stress values and positioned in the safety range [18]. Based on the thickness reduction results, it was shown that the use of single-stage wing holder design with a thickness of 10 mm instead of the current one is an important alternative in terms of simplifying the structure with complex geometry, reducing the thickness, and finally the cost.

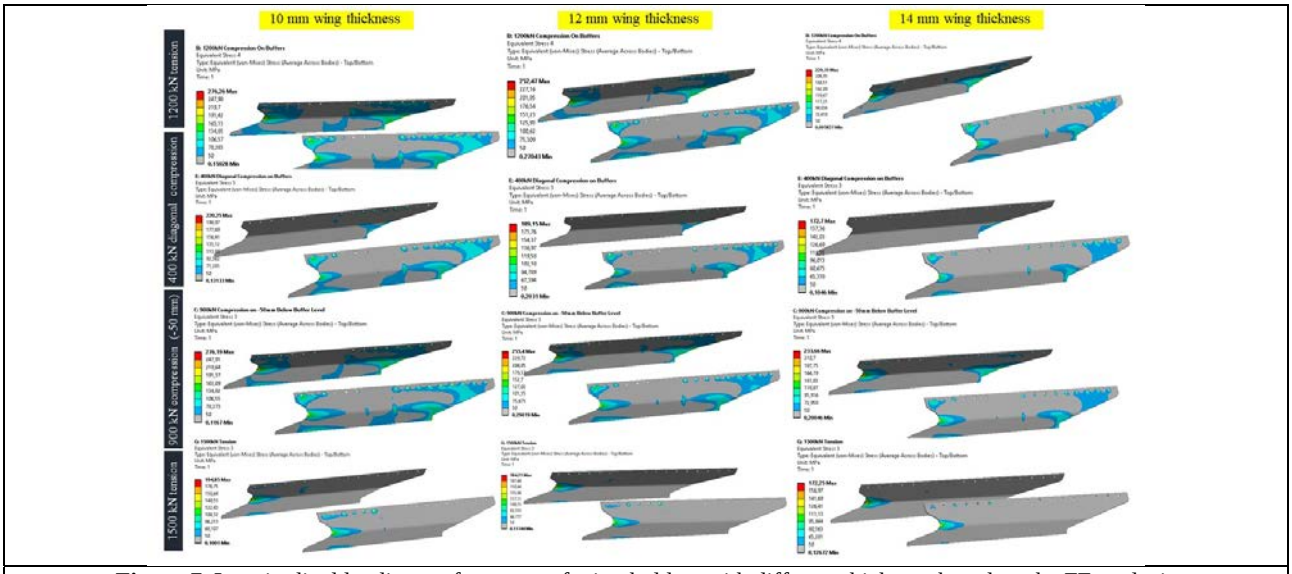



**Figure 7.** Longitudinal loading performance of wing holders with different thickness based on the FE analysis

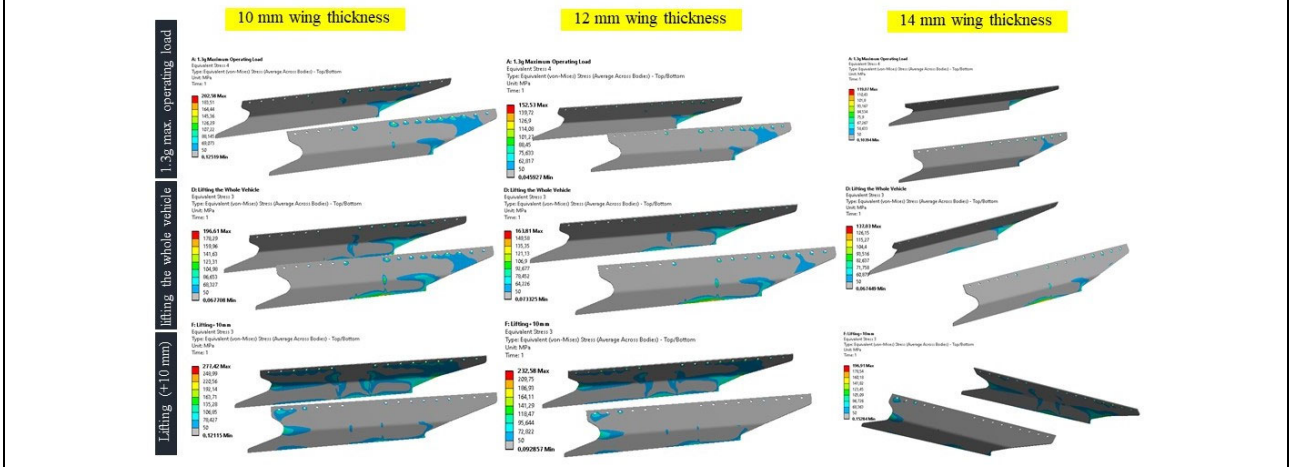



**Figure 8.** Vertical loading performance of wing holders with different thickness based on the FE analysis

## 4. CONCLUSIONS

According to the finite element analysis and thickness reduction process for the wing holders of tank wagons, following conclusions could be drawn:

• The maximum von Mises stress in the entire wagon system and particularly in the wing holders was observed to be lower than the safety stresses specified in the standard .

• Regarding the longitudinal loading conditions applied to the connecting different wing holders, the total deformations were within the deformation limits specified in the standard.

• In longitudinal loading conditions, the most critical zones were around the tank cap and the bolt-nut connection zones of the retainer wing holders and the bending zones, whereas the corner positions of the wing holders were detected as the most critical zone in vertical loading condition.

• The middle and side areas of the tank and the bogie enclosures were found to be the safer zones in the loadings. The most effective loading types on wing holders were determined as 900 kN compression (-50 mm) under longitudinal loading and whole vehicle lift (+10 mm location) under vertical loading conditions .

• The main goal of this research, i.e., wing holder thickness reduction, was realized, and significant improvements in terms of assembly cost and production cost will be achieved by this simple and single-stage design.

## ACKNOWLEDGMENTS

The authors wish to thank FE-TECH Company for conducting the finite element analysis.

## CONFLICT OF INTEREST

The authors declare no conflict of interests in this work.

## REFERENCES

1. O. Fomin, A. Lovska, P. Kučera, V. Píštěk, Substantiation of Improvements for the Bearing Structure of an Open Car to Provide a Higher Security during Rail/Sea Transportation, Journal of Marine Science and Engineering 9(8) (2021) 873, https://doi.org/10.3390/jmse9080873.

2. A. Lovska, O. Fomin, V. Píštěk, P. Kučera, Dynamic Load and Strength Determination of Carrying Structure of Wagons Transported by Ferries, Journal of Marine Science and Engineering 8(11) (2020) 902, https://doi.org/10.3390/jmse8110902.

3. L. Vukić, I. Kraemer, Dependence of Transport and External Cost Variables on Transportation Route Length, Journal of Marine Science and Engineering 9(11) (2021) 1270, https://doi.org/10.3390/jmse9111270.

4. A. Sulym, P. Khozia, E. Tretiak, V. Píštěk, O. Fomin, P. Kučera, Aspects of Strength Testing of Tank Containers in Compliance with the Requirements of the UN Navigation Rules and Regulations, Journal of Marine Science and Engineering 9(3) (2021) 349, https://doi.org/10.3390/jmse9030349.

5. S. Zhu, X. Xu, Y. Li, Dynamic response of railway vehicle with aerodynamic admittance function: An optimized algorithm, Journal of Wind Engineering and Industrial Aerodynamics 227 (2022) 105075, https://doi.org/10.1016/j.jweia.2022.105075.

6. Y. Guo, Q. Sun, Y. Sun, Dynamic evaluation of vehicle-slab track system under differential subgrade settlement in China's high-speed railway, Soil Dynamics and Earthquake Engineering 164 (2023) 107628, https://doi.org/10.1016/j.soildyn.2022.107628.

7. J.Y. Alcaraz, J. Zhang, A.P. Nagalingam, S.K. Gopasetty, B.L. Toh, A. Gopinath, K. Ahluwalia, M.G.W. Ang, S.H. Yeo, Numerical modeling of residual stresses during vibratory peening of a 3-stage Blisk – a multi-scale discrete element and finite element approach, Journal of Materials Processing Technology 299 (2022) 117383, https://doi.org/10.1016/j.jmatprotec.2021.117383.

8. Y. Bai, Z. He, C. Su, N. Bao, H. Wang, G. Shi, Y. Wang, J. Yun, Z. Wang, Research on dynamic characteristics of novel filled damping block mesh-type rail pads for heavy haul railways, Construction and Building Materials 354 (2022) 129174, https://doi.org/10.1016/j.conbuildmat.2022.129174.

9. C. Qu, Z. Wang, L. Wei, Y. Xiao, Z. Chang, Field investigation of dynamic responses of a culvert-embankment transition zone in high-speed railway, Soil Dynamics and Earthquake Engineering 158 (2022) 107314, https://doi.org/10.1016/j.soildyn.2022.107314.

10. G. Song, H. Ji, W. Pei, J. Li, J. Zhao, W. Xiao, B. Wang, Prediction of microstructure evolution during multidirectional forging of the railway wagon bogie adpter, Materials Today Communications 32 (2022) 104143, https://doi.org/10.1016/j.mtcomm.2022.104143.

11. O. Fomin, J. Gerlici, A. Lovska, M. Gorbunov, K. Kravchenko, T. Lack, Creating mathematical model of the bearing structure dynamic load of the flat wagon from round pipes in the main operational modes, Transportation Research Procedia 55 (2021) 875-881, https://doi.org/10.1016/j.trpro.2021.07.179.

12. J. Kim, J. Yoon, B. Kang, Finite element analysis and modeling of structure with bolted joints, Applied Mathematical Modelling 31(5) (2007) 895-911, https://doi.org/10.1016/j.apm.2006.03.020.

13. C. Chang, L. Ling, S. Chen, W. Zhai, K. Wang, G. Wang, Dynamic performance evaluation of an inspection wagon for urban railway tracks, Measurement 170 (2021) 108704, https://doi.org/10.1016/j.measurement.2020.108704.

14. E. Kuba, M. Moravčík, V. Pavelčík, Experimental verification of tank wagon's ability to transmit longitudinal forces in opposite track curves, Transportation Research Procedia 55 (2021) 774-781, https://doi.org/10.1016/j.trpro.2021.07.045.

15. J. Gerlici, Y. Fomina, O. Fomin, K. Kravchenko, V. Hauser, Analysis of the possibility of the use of tough side bearers in the covered wagons design for the light-weight loads transportation, Transportation Research Procedia 40 (2019) 694-702, https://doi.org/10.1016/j.trpro.2019.07.098.

16. T. Jin, Z. Liu, S. Sun, Z. Ren, L. Deng, B. Yang, M.D. Christie, W. Li, Development and evaluation of a versatile semi-active suspension system for high-speed railway vehicles, Mechanical Systems and Signal Processing 135 (2020) 106338, https://doi.org/10.1016/j.ymssp.2019.106338.

17. R. Xiu, M. Spiryagin, Q. Wu, S. Yang, Y. Liu, Fatigue life assessment methods for railway vehicle bogie frames, Engineering Failure Analysis 116 (2020) 104725, https://doi.org/10.1016/j.engfailanal.2020.104725.

18. S.S. Harak, S.C. Sharma, S.P. Harsha, Structural Dynamic Analysis of Freight Railway Wagon Using Finite Element Method, Procedia Materials Science 6 (2014) 1891-1898, https://doi.org/10.1016/j.mspro.2014.07.221.

19. K. Kravchenko, P. Šťastniak, M. Moravčík, J. Dižo, M. Blatnický, An innovative design of a protective device for integrity of tank wagons in a collision, Transportation Research Procedia 55 (2021) 767-773, https://doi.org/10.1016/j.trpro.2021.07.044.

20. G. Vatulia, A. Falendysh, Y. Orel, M. Pavliuchenkov, Structural Improvements in a Tank Wagon with Modern Software Packages, Procedia Engineering 187 (2017) 301-307, https://doi.org/10.1016/j.proeng.2017.04.379.

21. O. Fomin, A. Lovska, V. Bohomia, I. Berestovoi, Determination of dynamic loading of a tank wagon with malleable links between the pot and the frame, Procedia Structural Integrity 36 (2022) 239-246, https://doi.org/10.1016/j.prostr.2022.01.030.

22. A. Tevlek, H.M. Aydin, E. Maleki, R. Varol, O. Unal, Effects of severe plastic deformation on pre-osteoblast cell behavior and proliferation on AISI 304 and Ti-6Al-4V metallic substrates, Surface and Coatings Technology 366 (2019) 204-213, https://doi.org/10.1016/j.surfcoat.2019.03.034.

23. A. Colaço, A. Castanheira-Pinto, P. Alves Costa, J. Fernández Ruiz, Combination of experimental measurements

and numerical modelling for prediction of ground-borne vibrations induced by railway traffic, Construction and Building Materials 343 (2022) 127928, https://doi.org/10.1016/j.conbuildmat.2022.127928.

24. L. Zou, L. Lu, Y. Li, K. Yang, H. Zhao, Y. Dong, D. Zeng, Experimental and numerical study on press-fitted railway axles: Fretting fatigue behaviour in the very high cycle regime, International Journal of Fatigue 166 (2023) 107243, https://doi.org/10.1016/j.ijfatigue.2022.107243.

25. M. Živković, V. Milovanović, N. Jovanović, M. Bojović, Experimental and numerical investigation of sliding bolt connection on the wagon for the transport petroleum products, Materials Today: Proceedings 32 (2020) 88-92, https://doi.org/10.1016/j.matpr.2020.02.819.

26. Z. Song, S. Fang, Y. Zhang, J. Xie, Cracking analysis of bolster cover plate in C70 freight wagons, Engineering Failure Analysis 30 (2013) 43-60, https://doi.org/10.1016/j.engfailanal.2012.12.015.

27. E. Maleki, D. Burton, M.C. Thompson, On the flow past and forces on double-stacked wagons within a freight train under cross-wind, Journal of Wind Engineering and Industrial Aerodynamics 206 (2020) 104224, https://doi.org/10.1016/j.jweia.2020.104224.